Int. J. Morphol.,
42(4):1080-1095, 2024.

The Role of Marein During Endothelial–Mesenchymal Transition in Diabetic Kidney Disease

Rol de la Mareína Durante la Transición Endotelial-Mesenquimatosa en la Enfermedad Renal Diabética

Fang Zhang[1]; Qiong Guo[1]; Gulnigar Mamat[1]; Yating Tian[1]; Qiuyu Wang[2]; Boxiang Zhang[3] & Tian Li[1]

ZHANG, F.; GUO, Q.; MAMAT, G.; TIAN, Y.; WANG, Q.; ZHANG, B. & LI, T. The role of marein during endothelial–mesenchymal transition in diabetic kidney disease. *Int. J. Morphol., 42(4)*:1080-1095, 2024.

SUMMARY: Marein is a flavonoid compound that reduces blood glucose and lipids and has a protective effect in diabetes. However, the effect and mechanism(s) of marein on renal endothelial–mesenchymal transition in diabetic kidney disease (DKD) have not been elucidated. In this study, single-cell sequencing data on DKD were analyzed using a bioinformation method, and the data underwent reduced dimension clustering. It was found that endothelial cells could be divided into five subclusters. The developmental sequence of the subclusters was 0, 1, 4, 2, and 3, of which subcluster 3 had the most interstitial phenotype.The expression of mesenchymal marker protein:Vimentin(VIM), Fibronectin(FN1), and fibroblast growth factor receptor 1 (FGFR1) increased with the conversion of subclusters. In db/db mice aged 13–14 weeks, which develop DKD complications after 8–12 weeks of age, marein reduced blood levels of glucose, creatinine, and urea nitrogen, improved structural damage in kidney tissue, and reduced collagen deposition and the expression of FN1 and VIM. Marein also up-regulated autophagy marker:Light chain 3II/I(LC3II/I) and decreased FGFR1 expression in renal tissue. In an endothelial–mesenchymal transition model, a high glucose level induced a phenotypic change in human umbilical vein endothelial cells. Marein decreased endothelial cell migration, improved endothelial cell morphology, and decreased the expression of VIM and FN1. The use of the FGFR1 inhibitor, AZD4547, and autophagy inhibitor, 3-Methyladenine(3-MA), further demonstrated the inhibitory effect of marein on high glucose–induced endothelial–mesenchymal transition by reducing FGFR1 expression and up-regulating the autophagy marker protein, LC3II/I. In conclusion, this study suggests that marein has a protective effect on renal endothelial–mesenchymal transition in DKD, which may be mediated by inducing autophagy and down-regulating FGFR1 expression.

KEY WORDS: Endothlial-mesenchymal transition; Marein; Diabetic kidney disease; FGFR1; Autophagy.

INTRODUCTION

Diabetic kidney disease has become a global public health problem. Diabetic kidney disease (DKD) is a common and serious complication of diabetes, which is mainly manifested by progressive proteinuria and renal function decline, and eventually develops into end-stage renal disease, requiring dialysis or kidney transplantation, which seriously threatens the life and health of patients and occupies a large number of social and medical resources (DeFronzo *et al*., 2015; Kalantar-Zadeh *et al*., 2021). Therefore, efforts to achieve effective prevention and treatment of diabetic nephropathy is an urgent problem in the field of medical and health care. The research and development of new anti-diabetic nephropathy drugs has become a research hotspot at present (Reidy *et al*., 2014).

Renal micro vessels are widely distributed and have abundant blood flow. When the kidney is in a stressful environment such as high glucose and insulin resistance for a long time, vascular endothelial cells will be first stimulated and the metabolic pathway homeostasis of endothelial cells will be disturbed. Endothelial cells will lose endothelial phenotype and transform into mesenchymal phenotype, that is endothelium-mesenchymal transition (EndMT), accelerating the generation and development of local kidney

[1] Department of Histology and Embryology, School of Basic Medical Sciences, Xinjiang Medical University, Urumqi Xinjiang, 830011, China.
[2] Department of Pharmacology, Pharmacy College, Xinjiang Medical University, Urumqi Xinjiang, 830011, China.
[3] The Second Clinical College of Medicine, Xinjiang Medical University, Urumqi Xinjiang, 830011, China.
FUNDING. The research was supported by the Xinjiang Uygur Autonomous Region University Research Program (XJEDU2020Y021); Doctoral Initiation Fund;National Innovation and Entrepreneurship Training Program for College Students (202010760011) and the Natural Science Foundation of Xinjiang Uygur Autonomous Region (No. 2018D01C181).

Received: 2024-04-05 Accepted: 2024-05-05

lesions (Barry *et al*., 2019; Lassén & Daehn, 2020; Dumas *et al*., 2021). Using the renal endothelial cell lineage tracing technique to study cell fate and tissue development, the results showed that endothelial cell derived myoblasts expressing a-SMA were present in the renal interstitium of streptozotocin (STZ) -induced diabetic nephropathy mice. This suggests that endothelium-mesenchymal transition of the renal endothelium promotes the generation and development of diabetic kidney disease (Jourde-Chiche *et al*., 2019; Kuppe *et al*., 2021; Xu *et al*., 2021). In addition, studies have proved that EndMT is a dynamic transition process, and the phenotype of this intermediate trans differentiation stage is unstable, which can be reversed by external intervention, so it becomes a potential target for treatment of related diseases (Baslan & Hicks, 2017; Wilson *et al*., 2019; Chen *et al*., 2019; Saelens *et al*., 2019). However, this issue has not been studied in diabetic nephropathy. Therefore, single cell sequencing data of diabetic nephropathy were obtained from a public database: Bioinformatics was used to investigate the mechanism of endothlial-mesenchymal transition in diabetic nephropathy.

Marein is a kind of flavonoid compound, extracted from the rare high-cold and unique Xinjiang special medicine two-color chrysanthemum, which can reduce blood glucose and blood lipid, effectively inhibit gluconeogenesis and improve insulin resistance (Dias *et al*., 2010, 2012). Current research results have proved that Marein can improve insulin resistance of human glomerular vascular endothelial cells induced by high glucose, reduce blood glucose and insulin levels in diabetic mice, and has potential application value in improving and delaying the disease course of diabetes and its complications (Niu *et al*., 2021). However, the effect of Marein on renal endothlial-mesenchymal transition in diabetic kidney disease, and the key molecular mechanisms have not been studied. Previous network pharmacological studies have found that Marein has a strong interaction with FGFR1, suggesting that FGFR1 may be a key molecule in the role of Marein in DKD (Li *et al*., 2022). Therefore, in this study, the single cell sequencing data of diabetic nephropathy from open database was used for bioinformatics analysis, combined with *in vivo* and *in vitro* experiments?to study the effect and mechanism of Marein on endothlial-mesenchymal transition in diabetic kidney disease.

MATERIAL AND METHOD

Data source. Single-cell RNA sequencing data were downloaded from the GEO database (GSE131882) from kidney tissue samples from kidney resection (each patient signed an informed consent and the experiment was approved by the Biomedical Research Ethics Committee of Southern Denmark in accordance with the Declaration of Helsinki). The 3 samples with the most comprehensive data were selected from the normal group and the disease group, and bioinformatics analysis was conducted on the sequencing data of the samples.

Data preprocessing. FASTQ files are decoded, aligned, quality filtered, and UMI counted via CellRanger v3.0. According to the similar expression profile of DropletUtils packaged environmental solution, the empty droplet data were detected and removed. Potential doublet cells were identified using the doublet score calculated by the scan packet function doublet cells and excluded from the downstream analysis. Low-expression genes and low-quality cells were excluded according to the following criteria: (1) genes expressed in fewer than 3 cells, (2) cells expressed in 200 or less genes or more than 3,500 genes, and (3) cells expressed in genes with 0.10 percentage of mitochondria.

Data standardization and batch calibration. After quality control, the SCTransform function was used for data normalization, variable feature detection and data scaling. It then applies FindIntegrationAnchors and IntegrateData functions to identify anchors and consolidate data sets to eliminate batch effects between samples.

Dimensionality reduction clustering. In order to reduce the dimension, RunPCA function was used for principal component analysis, and the first 30 PCS were selected to construct the common nearest neighbor graph of the low-dimensional subspace. After clustering the cells by the FindClusters function with a resolution of 0.2, use the RunTSNE function for nonlinear dimensionality reduction.

Cell type identification and analysis. Cell types were identified according to the typical genetic markers of the renal cortex and classified into corresponding clusters. The percentage of cell types in each group was calculated and a barplot was formed using the ggplot2 function.

Cell subpopulation identification. The UMI count matrix is loaded into the R package, and Seurat objects are created using the Seurat package to identify cell subsets based on shared nearest neighbor (SNN) clustering algorithms. Subgroups were identified using analysis of variance (ANOVA) to determine the markers that best distinguish different subgroups.

Trajectory inference analysis. Pseudo-time trajectory analysis uses Monocle2 to infer pseudo-time trajectory. Seurat objects are converted into unit data set objects, and DDRTree method is used for dimension reduction. The orderCells function was used for pseudo-time sorting and the plot_cell_trajectory function was used to visualize the

results. ggplot2 scatter plot was used to show the change of gene expression with pseudo time.

Identification of differentially expressed genes. In order to explore the differences between different groups and different subgroup transcriptomes, findmarker function was used to identify differentially expressed genes (DEGs). The molecular regulatory heat maps of different cell subpopulations were generated using the dotplot and pheatmap functions respectively.

Animal feeding and group administration. Male db/m mice aged 5-6 weeks in control group and db/db mice in model group were purchased from Changzhou Cavence Laboratory Animal Co.LTD. The mice were kept in SPF animal feeding room of Animal Experimental Center.Xinjiang Medical University, and were tested in accordance with the Guidelines for the Care and Use of Experimental Animals of Xinjiang Medical University, approval number: IACUC-20190226-20. Ten db/m mice were used as the normal control group, and 30 db/db mice were divided into model group (n=10), Metformin (MedChem Express,lot#29902)positive group (n=10;280 mg/kg), and Marein (Extrasynthese) administration group (n=10;50 mg/kg) according to random number table method. The volume of the mice was 0.2 mL/10 g by intragastric administration. The mice lasted for 8 weeks and reached the age of 13-14 weeks.

Biochemical index detection. Mouse tail blood samples were taken at designated time, blood beads were drawn from blood glucose strips, and fasting blood glucose levels (FBS) of mice were detected by glucose meter (Roche Diabetes Care GmbH). Blood samples were collected from mouse eyeballs for the detection of creatinine (BUN) and urea nitrogen (Scr) biochemical indices(Jiangsu Meibiao Biotechnology Co.,Ltd. S05027-2 and S0131O-2).

Hematoxylin and eosin (H&E) staining. Mouse kidney tissue was immersed in 4 % paraformaldehyde for paraffin embedding. The tissue wax block was cut into 5mm thickness slices. Dewaxing and rehydrating were performed. Paraffin sections were placed in xylene I and xylene II for 20min, and then immersed in anhydrous ethanol, 95 % alcohol I, 95 % alcohol II and 80 % alcohol successively for 5s. The sections were immersed in hematoxylin dye solution for 5min and acid eosin dye solution for 1min, then washed with tap water until colorless?biosharp,Cat.NO.:BL700B. Dehydration clear, in the order of 80 % alcohol, 95 % alcohol I, 95 % alcohol II, anhydrous ethanol, xylene I and xylene II. The slices were dried and sealed with resin. The images were observed under a photographic microscope (LeicaDM3000).

Masson staining. Sections were dewaxed and rehydrated. The staining was followed by iron hematoxylin staining for 5min, lichun red staining for 5min and aniline blue staining(Cat#G1340;Solarbio). The control time of aniline blue staining was the same in each group, and the staining was terminated by rinsing with distilled water. Then it was dehydrated with 95 % ethanol for 2s. Finally, the sections were differentiated in xylene I and xylene II, and the sections were dried and resin sealed to be solidified. The images were observed under a photographic microscope, and the Image J software was used for semi-quantitative analysis.

Immunohistochemical(IHC) staining. The slices were dewaxed and rehydrated, and then repaired with citrate antigen (Beijing Zhong Shan-Golden Bridge Biologicaln Technology Co., Ltd). The slices were boiled at high heat in microwave oven for 5 min and cooled to room temperature. The tissues were covered with goat serum (ZLI-9002; Beijing Zhong Shan-Golden Bridge Biologicaln Technology Co., Ltd) and incubated at 37 °C for 1 h. The covered tissue of Fibronectin and Vimentin (FN1 and VIM; ab2413 and ab137321; dilution both are 1:500, abcam) primary antibody was diluted with antibody diluent (ZLI-9028; Beijing Zhong Shan-Golden Bridge Biologicaln Technology Co., Ltd) and incubated overnight in 4 °C refrigerator. The next day, the wet box equalized room temperature for 45 min. The tissues were covered with immunohistochemical secondary antibodies (PV-6000; Beijing Zhong Shan-Golden Bridge Biologicaln Technology Co., Ltd) and incubated at 37 °C for 30 min. Then DAB color development was performed (ZLI-9018; Beijing Zhong Shan-Golden Bridge Biologicaln Technology Co., Ltd). When there was obvious positive expression of brown, the section was immersed in tap water to terminate color development. Dip the sections into the hematoxylin dye solution for 25 s and rinse the sections with running water until no color is found. Then dehydration and transparency were carried out, and the slices were dried and sealed with resin. Images were observed and taken under a microscope. Image J software was used for semi-quantitative analysis.

Transmission electron microscopy(TEM) observation. Kidney tissue blocks were cut to the size of 1 MM to the third, and 2.5 % glutaraldehyde was fixed overnight. Wash with phosphoric acid bleach solution 3 times for 15 min each time, fix with 1 % osmic acid fixative solution for 3 h, and then wash with phosphoric acid bleach solution 3 times for 15min each time. Then, dehydration was carried out in the refrigerator at 4 °C for 15 min of 50 % ethanol, 15 min of 70 % ethanol, 15 min of 90 % ethanol, 15 min of 90 % ethanol and 90 % acetone 1:1 mixture, 20 min of 90 % acetone, and finally at room temperature for 15 min of 100 % acetone. The tissue blocks were immersed in the embedding solution

at room temperature for 4 hours, and then cured and placed in the oven at 60? for 24 hours. The tissue blocks were cut into 50-60nm slices using an ultra-thin microtome. 3 % uranium acetate - lead citrate double staining, and finally transmission electron microscope observation and photography (JEM-F200;JEOL).

Cell culture and grouping. Human umbilical vein endothelial cells (HUVEC) were purchased from Guangzhou Genio Biotechnology Co., LTD. HUVEC cells were cultured in an incubator at 37 °C and 5 % CO_2, and operated in an ultra-clean aseptic environment. The cell culture medium consisted of 10 % FBS(Lot:2282897RP;Gibco),1 % penicillin streptomycin double antibody solution(BJ111995904;Biosharp), and high glucose DMEM(AH29882654;Global Life Sciences Solutions USA LLC) base medium. Grouping and administration methods: 1. Cells were divided into normal group and model group (50 mmol/L; 48 h), positive drug Metformin group (100 μM), Marein low-dose group (10 μM), Marein medium-dose group (40 μM) and Marein high-dose group (160 μM). 2. Cells were divided into normal group and model group (50 mmol/L; 48 h), AZD4547(CAS NO:1035270393; MedChemExpress) intervention group (1 μM), high dose of Marein (160 μM), AZD4547 (1 μM) and high dose of Marein (160 μM) combined intervention group, and 3-MA (5 mM) (CAS NO:5142234; MedChemExpress) and high dose of Marein (160 μM) combined intervention group. When a combination of inhibitors (AZD4547, 3-MA) and Marein was used to intervene cells, the inhibitor was administered 2 h before administration.

CCK8 test. Pancreatic enzymes digested the cells and counted them, adding them into 96-well plates at a concentration of 5×10^4 cells/ml, 100μl per well. High sugar was diluted into 10 mM, 20 mM, 30 mM, 40 mM and 50 mM by base medium. The concentration of Marein was diluted into 1 μM, 5 μM, 10 μM, 20 μM, 40 μM, 80 μM, 160 μM, 240 μM, and the cells were treated for 24 and 48h. Add 100 ul of CCK8 (ba00208; Bioss) to each well and incubate for 2 h. The absorbance of each well was measured by enzymoleter at 450 nm wavelength, and the survival rate of different components was calculated.

The EndMT model was established by ELISA. The cells were inoculated into 6-well plates at the concentration of 5×10^6 cells /mL. The normal group was treated with high glucose DMEM basic medium, and the other components were treated with high glucose 10 mM, 20 mM, 30 mM, 40 mM and 50 mM, and the timing was 24 h and 48 h. The supernatant of cells in each group was absorbed and centrifuged at 12000 rpm for 20 min. After that, the concentration of type I collagen in the supernatant was detected according to the kit instructions (Cat No:JL19029; Shanghai Jianglai Biotechnology Co., Ltd.).

Cell morphology and scratch experiments. When the cells were grown and fused into monolayers, they were removed from the medium state and placed under a microscope to observe the morphology and photograph. A sterile pipette suction was used to scratch a line in the middle of the dish to create a blank area, then photographs were taken and time was recorded. After 48 h of cell culture, the cells were photographed again under the microscope to check the growth and migration of the cells to the blank area.

Western Blotting. The lysate PMSF and RIPA were configured in a ratio of 1:100 for cell lysis and protein extraction. The protein concentration of sample was obtained by BCA protein quantification method (Thermo Sciebtific; WK342259). 12.5 % SDS-PAGE gel was prepared (Biotides; WB2103). Add samples at 20 μg per well, and add 5 μL for Marker (Thermo; 91227189) per well. Set the condition as constant voltage, concentrated glue 80V, 30 min; Separation gel 120V, 60 min electrophoresis (PowerPac™ HC; Bio-Rad). The PVDF membrane(Millipore;48659900) is activated by methanol to prevent bubbles from forming and the membrane is tightly closed with the gel. Constant voltage 110V lasts for 90 min. 5 % milk seal 2h. The Fibronectin (abcam; ab2413),Vimentin (abcam; ab137321), Fibroblast Growth Factor Receptor I (Cell Signaling Technology; D8E4), LC3II/I(Cell Signaling Technology; 12741S) and GAPDH (Affinity; AF7021). Primary antibody incubation strips were incubated overnight in a shaker in a 4 °C refrigerator. Clean with 1×TBST (0.01 % Tween) for 3 times, and incubate the second antibody, IgG H&L/HRP (Bioss;bs40295G), against light for 50 min. Image J software was used for data analysis of strip gray values.

Statistical analysis. All the data were represented by mean ± standard deviation (). SPSS26.0 software was used for statistical analysis of the data of each group.Single-factor variance (ANOVA) analysis was used for statistical analysis of the data of multiple groups, and the test level $\alpha=0.05$. $P < 0.05$ indicated that the difference was statistically significant.GraphdPadPrism8.0 software assists in the production of statistical charts.

RESULTS

Bioinformatics analysis of single-cell sequencing data to predict the mechanism of renal endothelial–mesenchymal transition in diabetic nephropathy. In this study, endothelial cells (EC) were the main cell species of concern. The Findmarker function was used to identify differentially expressed genes (DEGs). A total of 26 DEGs were found in

control and DN groups. Of these, 10 genes were up-regulated and 16 genes were down-regulated in the DN group compared with the control group (Table I). Gene ontology gene functional enrichment analysis was performed on up-regulated genes in the DN group. Compared with the control group, up-regulated genes in the DN group were mainly genes related to cell proliferation, transcription and translation, apoptosis, and the inflammatory response (Fig. 1).

Table I. Differentially expressed genes between the two groups.

Gene Name	Expression	P-Value	-logFC
NR4A1	Up-regulated	8.60E-112	0.51858669
BHLHE40	Up-regulated	6.45E-80	0.384489227
IER3	Up-regulated	4.65E-60	0.352309392
FOS	Up-regulated	1.20E-52	0.316400624
ELF3	Up-regulated	2.72E-52	0.309666192
KLF6	Up-regulated	7.30E-46	0.466440958
PDE10A	Up-regulated	1.25E-42	0.363435391
VMP1	Up-regulated	2.74E-30	0.615010413
NFKBIZ	Up-regulated	1.34E-24	0.313491405
SGK1	Up-regulated	1.88E-12	0.329257947
MUC20-OT1	Down-regulated	2.09E-248	0.476774983
WNK1	Down-regulated	5.25E-127	0.575232381
PTH1R	Down-regulated	1.09E-87	0.381584809
FKBP5	Down-regulated	4.27E-83	0.506218529
MT-RNR2	Down-regulated	2.28E-72	0.309119926
CLCNKB	Down-regulated	1.04E-71	0.309969128
SLC12A3	Down-regulated	1.15E-71	0.871138597
TMEM101	Down-regulated	2.65E-67	0.329353104
FTCD	Down-regulated	5.54E-59	0.710858853
GPX3	Down-regulated	1.24E-58	0.427924276
AFM	Down-regulated	2.93E-42	0.329056692
MIOX	Down-regulated	6.71E-42	0.457983262
ACSM2B	Down-regulated	2.57E-31	0.454296499
PRODH2	Down-regulated	3.18E-31	0.401287668
TRPM7	Down-regulated	1.02E-28	0.416677263
CYP3A5	Down-regulated	1.09E-15	0.50981021

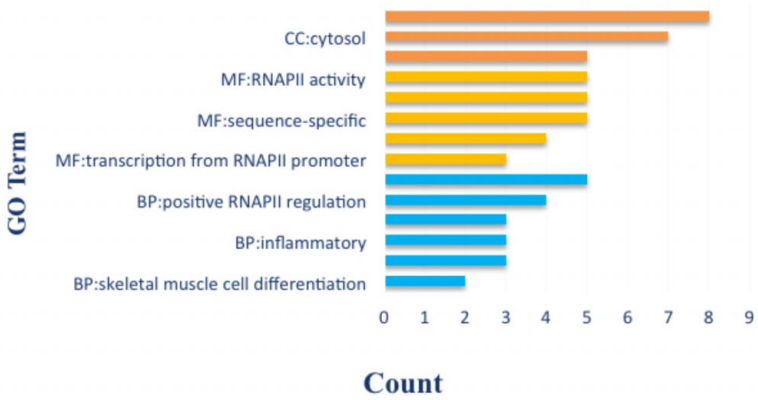

Fig. 1. GO functional enrichment analysis of differential genes "BP" refers to the biological process of the gene, "MF" refers to the molecular function expressed by the gene, and "CC" refers to the cellular component involved in the construction of the gene.

Using the RunPCA function for principal component analysis and FindClusters function for cell clustering, the data showed that kidney cells could be divided into 13 major categories (Fig. 2A). The classification of different cell populations is mainly based on the expression of marker genes of each cell population (Fig. 2C).

EndMT results in heterogeneity of the endothelial cell population in a dynamic transitional process. To explore the heterogeneity of endothelial cells in the DN kidney, a Seurat program was used to conduct unsupervised subclustering of endothelial cell clusters. It was found that endothelial cells could be further divided into five subgroups, namely 0, 1, 2, 3, and 4 (Fig. 2B). In order to explore whether the classifications and proportions of endothelial cell subsets in control and DN groups differed, a ggplot2 function was used to draw a bar chart of the proportion of endothelial cell subsets in the two groups (Fig. 2D). The proportion of endothelial cell subtype 0 was the largest in the control group, that of subtype 0 in the DN group was reduced, and those of subtypes 2 and 4 were significantly increased compared with the control group. In order to explore the relationship between different subgroups and help understand the differentiation and developmental process of the five subgroups of endothelial cells, we conducted pseudo-temporal developmental trajectory inference for subgroups (Fig. 2E). We found that with a development time from 0 to 10, the sequence of evolution of the corresponding subgroup was from subgroup 0 to subgroups 1, 4, 2, and 3, in that order. From the above developmental sequence, it was speculated that subpopulation 0 may have represented an endothelial cell population with a normal phenotype. Subgroups 1, 2, and 4 may have represented endothelial cell populations undergoing EndMT, of which subgroup 2 and finally subgroup 3 were closest to the mesenchymal cell phenotype. To further clarify the regulation of gene expression in endothelial cells during subpopulation transition, Seurat was used to make gene expression profiles of different subpopulations of endothelial cells during cell subpopulation transition (Fig. 3). A heatmap showed that gene expression changed with the development time of Pseudotime. The expression of FN1 and VIM also increased

during the transition of endothelial cells into subgroups 2 and 3. This again verifies that the subgroup transition of endothelial cells is closely related to the EndMT process, which is also consistent with previous speculation on findings.

The above studies indicated the existence of EndMT in the DN kidney. In order to explore the effect and mechanism of marein on DN kidney EndMT, we then elucidated the relationship between subgroup transition and the expression of FGFR1, a molecule that strongly interacts with marein (Fig. 2F). Scatterplot results showed that FGFR1 expression increased with the transition of endothelial cell subsets to mesenchymal phenotypic subsets 2 and 3; FGFR1 expression was highest in subgroup 2. These results suggest that the expression of FGFR1 in DN positively correlated with EndMT.

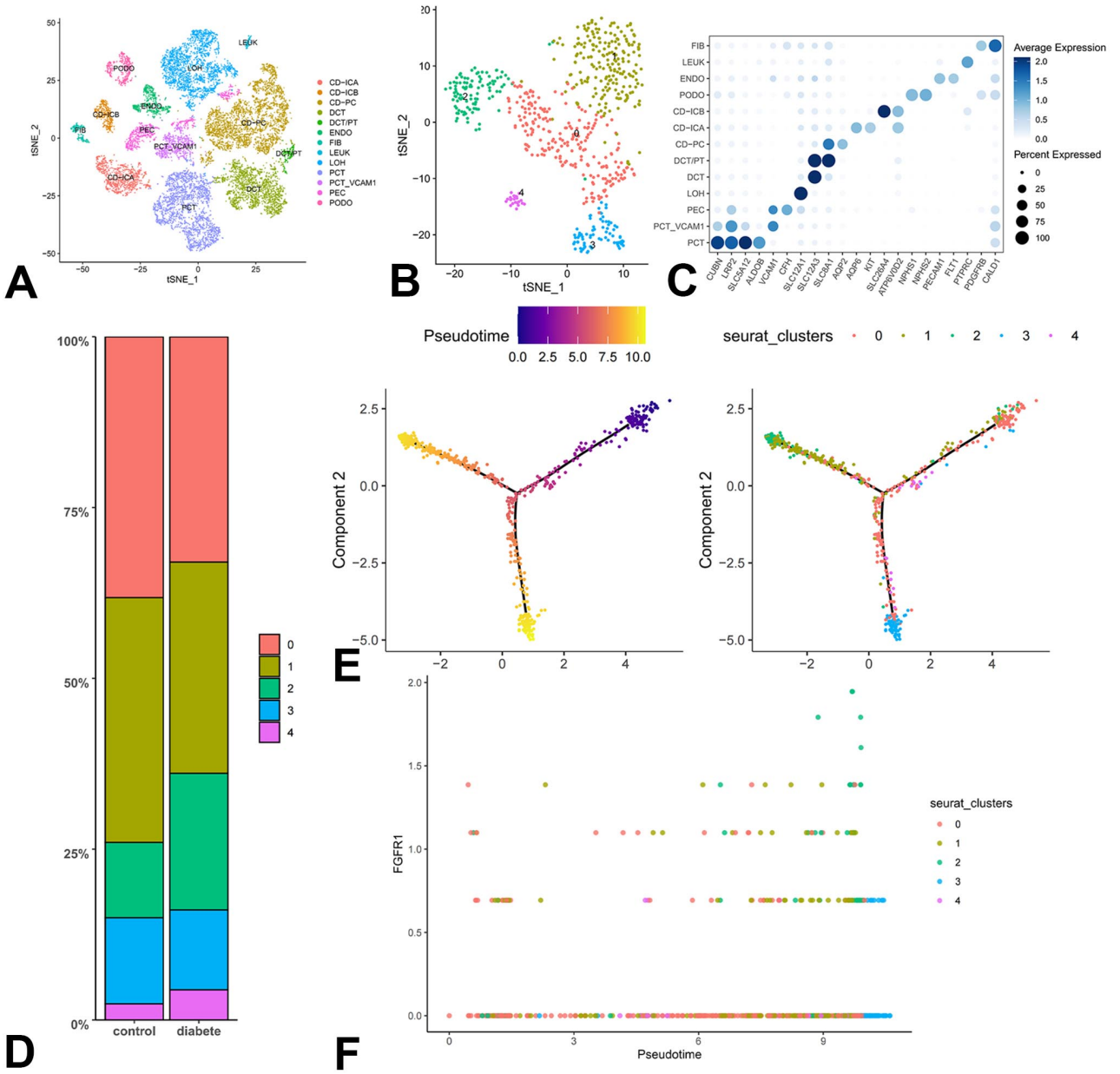

Fig. 2. The transition mechanism of EndMT in DN kidney was studied based on single-cell sequencing data analysis. (A) Dimensionality reduction cluster maps of kidney single cell sequencing data. (B) Subcluster classification of endothelial cells. (C) Marker genes of different cell types. (D) Bar charts of the proportion of different subclusters of endothelial cells between the two groups. (E) Pseudoradial developmental trajectory inference of endothelial subclusters. (F) Relationship between FGFR1 expression and endothelial subcluster transition.

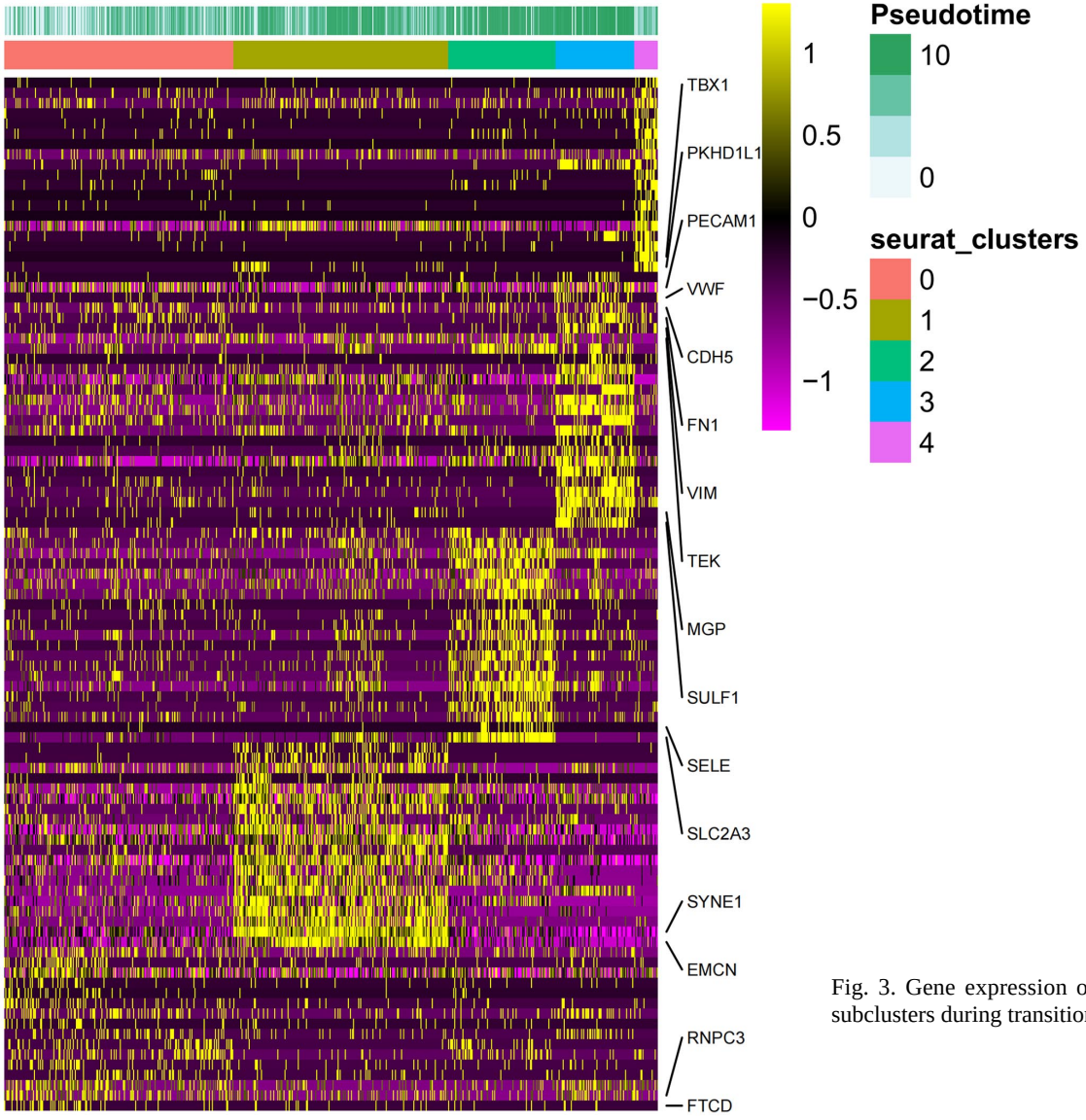

Fig. 3. Gene expression of endothelial cell subclusters during transition.

Effect of marein on EndMT in HUVEC induced by high glucose. In order to exclude the influence of different concentrations and times of high-sugar culture conditions on cell survival rate, a cell counting kit (CCK)8 assay was used to determine human umbilical vein endothelial cells (HUVEC) survival rates (Fig. 4A). We found that different concentrations of high glucose for 24 h and 48 h had no effect on cell survival rates. An enzyme-linked immunosorbent assay showed that compared with the untreated control cells, no significant difference was noted in the expression of type I collagen at a 10 mmol/L concentration of glucose; however, this was significantly increased at 20, 30, 40, and 50 mmol/L concentrations. The expression of type I collagen increased significantly at concentrations of 10, 20, 30 40, and 50 mmol/L of high glucose after 48 h (Fig. 4C). Based on the above experimental results, an EndMT model was established in endothelial cells after 48 h of intervention at 50 mmol/L of glucose.

A CCK8 assay showed that different concentrations of marein had no effect on cell survival rates (Fig. 4B). Therefore, a low dose of 10 μM, a medium dose of 40 μM, and a high dose of 160 μM of marein were selected as the conditions for cell intervention. To explore the effect of marein on EndMT induced by high glucose in endothelial cells, Western Blotting experiments showed that metformin and different concentrations of marein could reduce the expression of FN1 and VIM (Fig. 5A).Cell scratch test was

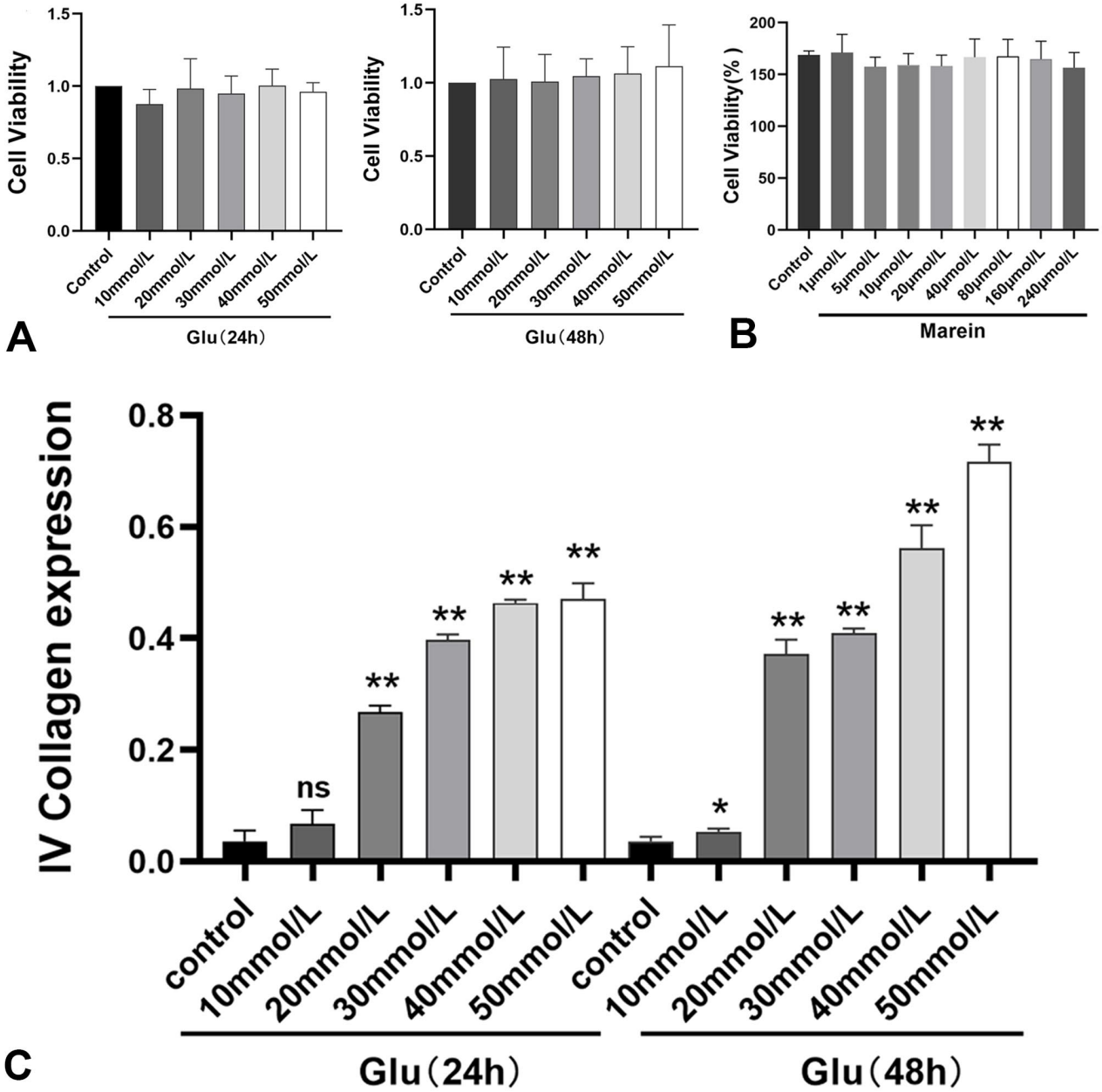

Fig. 4. Establishment of EndMT model of high glucose induced endothelial cells and screening of Marein administration concentration. (A) Effects of high glucose on survival rate of endothelial cells at 24 h and 48 h. (B) Effect of Marein on cell survival rate after 24 h. (C) ELISA was used to detect the expression of type I collagen in cells with different concentrations of high glucose. * compared with the normal group $P < 0.05$,** compared with the normal group $P < 0.01$, n=3.

employed that showed that the migration of endothelial cells treated with high glucose was significantly increased compared with the untreated cells. Migration by endothelial cells decreased after the intervention of metformin and different concentrations of marein (Figs. 5B and D). Observations of cell morphology showed that, compared with untreated cells, endothelial cells cultured under high glucose showed morphological changes, including fusiform fibroblasts. After the intervention of metformin and marein, the morphology of endothelial cells partially returned to an oval shape (Fig. 5C).

The mechanism of marein in EndMT induced by high glucose in endothelial cells. Western blotting showed that compared with untreated control cells, FGFR1 protein expression was increased and LC3II/I protein expression was decreased in the EndMT model group (Fig. 5E). After treatment with metformin, FGFR1 protein expression was

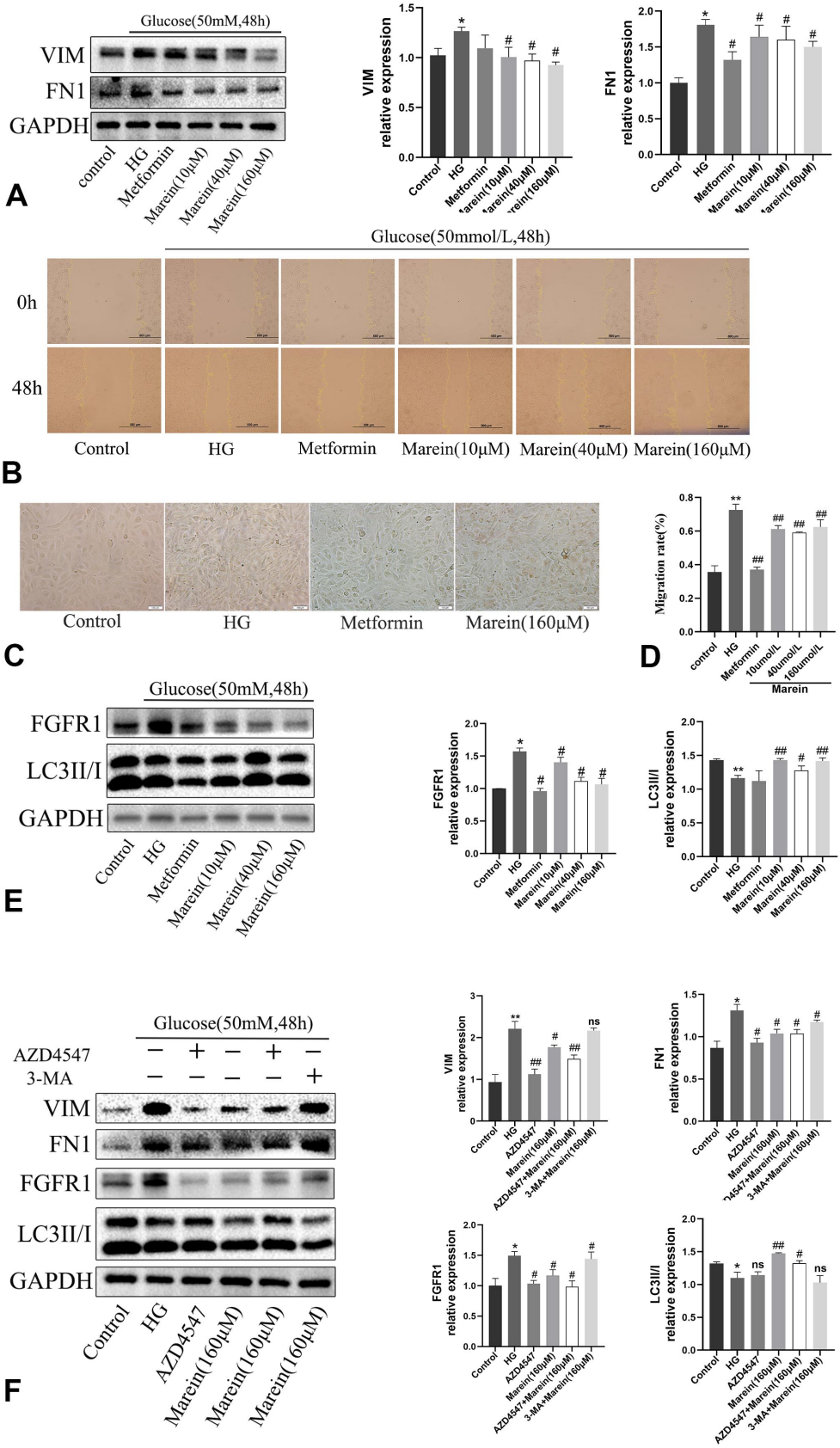

Fig. 5. Effect of Marein on EndMT induced by high glucose and its mechanism. (A) Effect of Marein on FN1 and VIM expression of EndMT in endothelial cells induced by high glucose.(B,D) Cell Marein ability was detected by scratch assay. (C) Morphological observation (E) Effect of Marein on the expression of FGFR1 and LC3II/I in hyperglycemic induced endothelial cells EndMT. (F) Study on the mechanism of the Marein effect on hyperglycemic induced endothelial cells EndMT .* compared with the normal group P < 0.05,** compared with the normal group P < 0.01,# compared with the model group P < 0.05, ## compared with the normal group P < 0.01,n=3.

Table IV-1 Results of FBG, SCR and BUN.

Groups	FBG（mmol/L）	SCR（μmol/L）	BUN（mmol/L）
db/m	6.38±0.68	768. 00±9.94	4.44±0.12
db/db	30.10±2.49**	2139.33±8.31**	9.54±0.19**
db/db+Metformin	26.12±3.26##**	1400.50±8.50##**	6.40±0.18##**
db/db+Marein	26.90±1.58#**	460.83±8.68#**	6.05±0.13#**

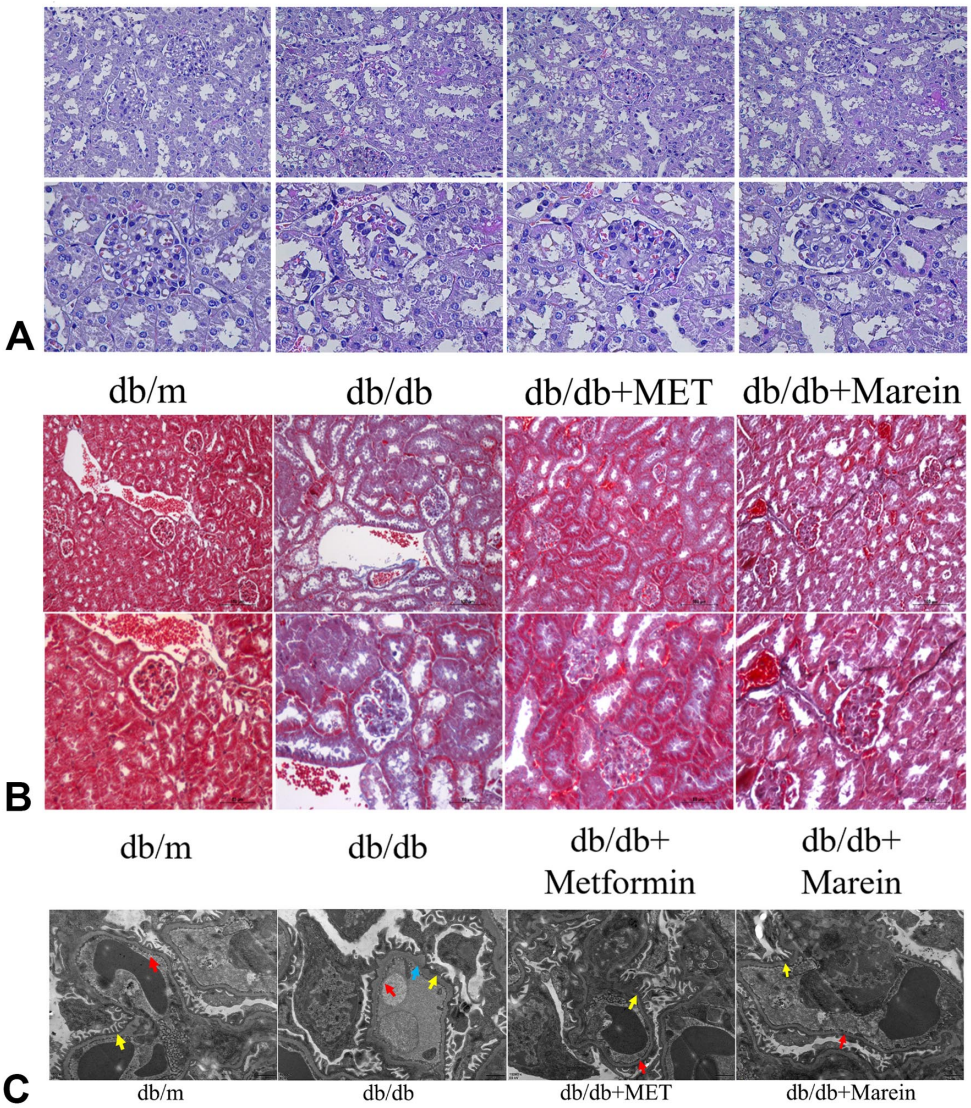

Fig. 6. Effects of Marein on kidney function and structure of db/db mice. (Table 6-1) Effects of Marein on fasting blood glucose (FBS), creatinine and urea nitrogen expression of db/db mice (A) Renal tissue structure of mice in each group was observed by HE staining (B) Collagen deposition in kidney of mice in each group was observed by Masson staining. (C) Transmission electron microscopy was used to observe ultrastructure of kidney tissue in each group of mice, Red arrows indicate endothelial cells; Yellow arrows indicate podocytes; Blue arrow indicates the basement membrane.* compared with the normal group $P < 0.05$,** compared with the normal group $P < 0.01$,# compared with the model group $P < 0.05$, ## compared with the normal group $P < 0.01$,n=6.

decreased. The expression of FGFR1 protein was decreased and the expression of LC3II/I protein was increased after intervention with different concentrations of marein. These results indicated that marein inhibited FGFR1 expression and up-regulated expression of the autophagy marker protein, LC3II/I. An FGFR1 inhibitor,AZD4547, and autophagy inhibitor, 3-MA, were used to help clarify the relationship between FGFR1 molecules, autophagy, and EndMT (Fig. 5F). We found that compared with EndMT model group, AZD4547 intervention inhibited FGFR1 protein expression while the expression of VIM and FN1 was decreased. Marein down-regulated FGFR1 expression and significantly decreased the expression of VIM and FN1, suggesting that marein exerts an inhibitory effect on endothelial–mesenchymal transition partly by inhibiting FGFR1 expression. When marein was combined with the autophagy inhibitor, 3-MA, compared with marein alone, marein lost its inhibitory effect on EndMT, FGFR1 expression was up-regulated, and VIM and FN1 expression was also increased. These findings suggest that marein may inhibit EndMT by inducing autophagy and inhibiting FGFR1 protein expression.

Effect and mechanism of marein on renal EndMT and fibrosis in db/db mice. The fasting blood glucose of mice in each treatment group was measured at the 8th week (Table 6-1). Compared with mice of the db/m group, fasting blood glucose levels of those in db/db, metformin, and marein groups were increased. Compared with mice of the db/db group, the fasting blood glucose in mice of the metformin-treated group was significantly decreased. The fasting blood glucose level of db/db mice in the marein-treated group was decreased, indicating that marein reduced the fasting blood glucose level. Creatinine test results showed that compared with db/m mice, the expression of creatinine in db/db and metformin-treated groups was increased, while that of mice in the marein-treated group was decreased. Compared with the db/db group, the creatinine levels of mice in metformin and marein groups were significantly decreased. In addition, compared with db/m mice, urea nitrogen levels in mice of db/db, metformin, and marein groups were significantly increased. Compared with mice of the db/db group, the urea nitrogen levels of mice in metformin and marein groups were significantly decreased. These results indicate that marein has a protective effect on kidney function in db/db mice.

The pathological structure of mouse tissues in each treatment group was also observed. Hematoxylin and eosin staining revealed that the kidney tissue structure of mice in the db/m group was clear and regular; the balloon cavity structure was clearly visible (Fig. 6A). In comparison, the renal tissue structure of diabetic db/db mice was damaged and the cytoplasm of renal tubular epithelial cells was loose and lightly stained. After db/db mice were treated with metformin and marein, kidney structure improved and the tissue structure was close to that of mice of the untreated control group. Masson staining was performed on the kidney tissues of mice in each group to detect collagen deposition (Fig. 6B). We found that compared with mice of the db/m group, collagen fiber expression in kidney tissue of mice in the db/db group was significantly increased; collagen fiber sites localized mainly in glomeruli and renal tubules. Metformin administration significantly reduced collagen deposition in db/db mice kidneys, and marein administration significantly reduced collagen fiber expression in the kidney tissue of db/db mice. The ultrastructure of kidney tissue was observed by transmission electron microscopy (Fig. 6C). The kidney podocytes in mice of the db/m group showed normal finger-like structures; glomerular endothelial cells had a window pore structure. The kidney tissue of db/db mice showed foot process fusion and decreased podocytes as well as decreased endothelial cell window pores and a thickened glomerular basement membrane. The administration of metformin led to an improvement in foot process fusion lesions, reduced endothelial cell window pores, and thickened basement membranes. After db/db mice were treated with marein, the finger protrusions of podocytes were restored, the window pores of endothelial cells increased, and the thickness of the basement membrane was restored to normal.

To detect the expression of FN1 and VIM in each group, immunohistochemical staining was conducted (Fig. 7A). Compared with db/m mice, FN1 expression in db/db mice was significantly increased; expression was mainly concentrated in the glomeruli and basement membrane of renal tubules. The expression of FN1 protein in the kidney tissue of db/db mice was significantly decreased after the administration of metformin and marein. The VIM expression of mice in each group was mainly concentrated in the glomerular vasculature and extra-glomerular mesangial region (Fig. 7B). Compared with mice in the db/m group, VIM expression in db/db mice was significantly increased. The expression of VIM in the kidney tissue of db/db mice was significantly decreased after the administration of metformin and marein.

Next, the effects of marein on LC3II/I and FGFR1 expression in the kidneys of db/db mice were investigated (Fig. 7C). Compared with untreated db/m mice, FGFR1 protein and gene expression in the kidney tissue of db/db mice was significantly increased, while LC3II/I protein expression was decreased. The expression of FGFR1 was decreased in the metformin group. The expression of FGFR1 was significantly decreased and the expression of LC3II/I was significantly increased in the marein group.

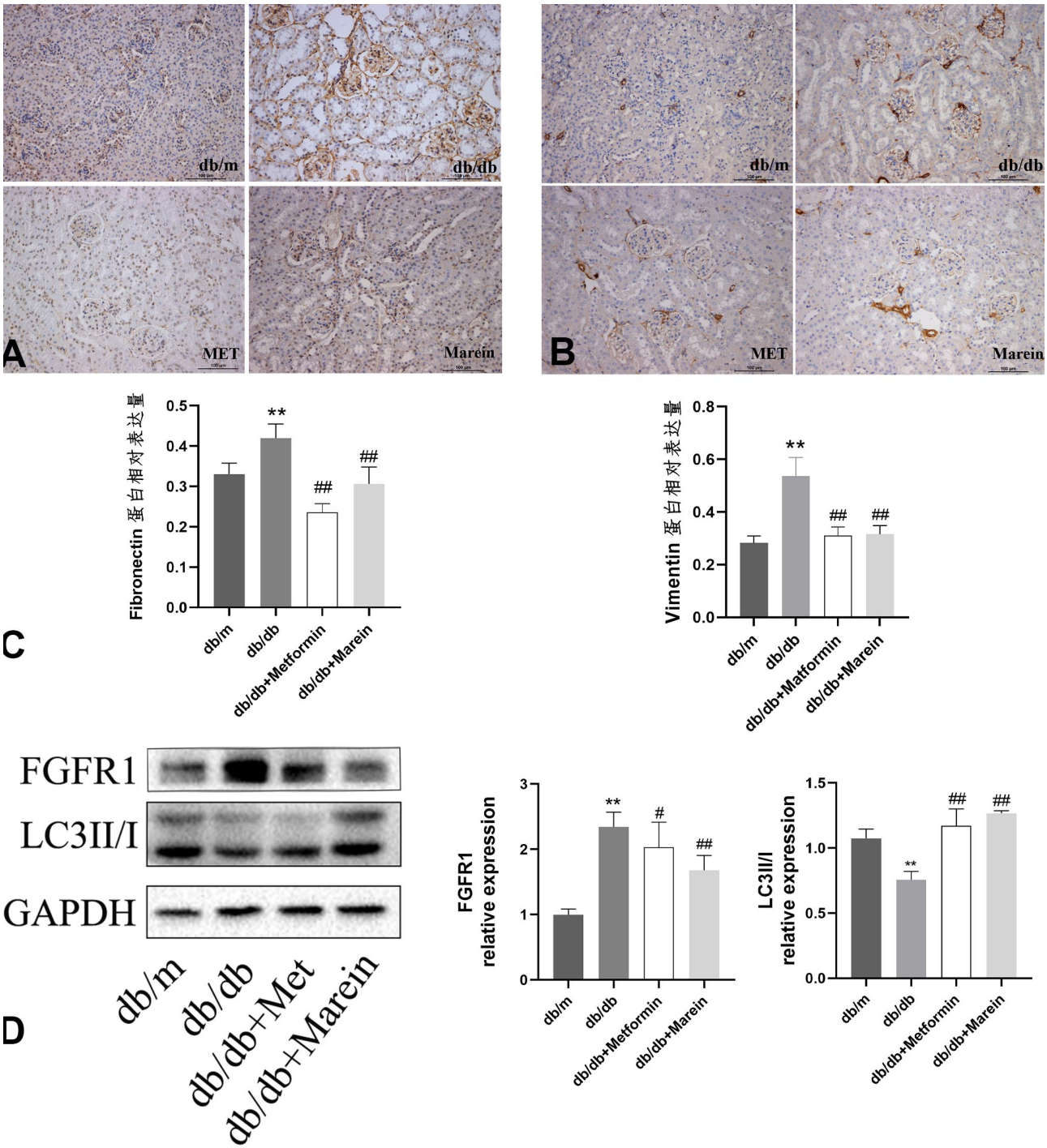

Fig. 7. Studies on EndMT in kidney tissue of db/db mice and its related mechanisms. (A) Positive expression of FN1 in kidney was detected by immunohistochemistry.(B) positive expression of VIM in kidney was detected by immunohistochemistry.(C) Effects of Marein on FGFR1 and LC3II/I expression in mice in each group.** compared with the normal group $P < 0.01$,# compared with the model group $P < 0.05$, ## compared with the normal group $P < 0.01$,n=6.

DISCUSSION

Diabetic nephropathy is the main cause of end-stage renal disease. Many different kinds of endothelial cells are distributed in the kidney and these play an important role in the transport of the kidney: glomerular endothelial cells are

involved in glomerular filtration; peritubular capillary endothelial cells are involved in secretion and reabsorption in renal tubules; and endothelial cells in the major renal veins and arteries are involved in maintaining blood circulation to the kidney (Gilbert, 2014; Jourde-Chiche *et al*., 2019). The hyperglycemic environment of DN first stimulates endothelial cells of the kidney that can promote the development of renal fibrosis and dysfunction by triggering EndMT (Chen *et al*., 2021; Kuppe *et al*., 2021). At present, the effective prevention and treatment of renal EndMT in DN remain to be further explored. Marein is a type of flavonoid monomer extracted from two-color *Chrysanthemum*, a characteristic medicine of Xinjiang. Previous studies have demonstrated that the flavonol extract of bicolor *Chinchilla* inhibits fibrotic changes induced by high glucose in rat glomerular mesangial cells (HBZY-1) cells by reducing the proteins expression of FN1, transforming growth factor (TGF)-β, and Smad2, P-Smad2, Smad4, and NADPH oxidase 4 in induced by high glucose (Yao *et al*., 2019). In addition, previous studies on the effects of marein showed that it reduced the expression of FN1 and type I collagen in human renal tubular epithelial cells (HK-2) cultured in high glucose (Guo *et al*., 2020). In addition, marein has a protective effect on inflammation and injury in HUVEC induced by a high sugar level (Wang *et al*., 2018). However, the effect of marein on the endothelial interstitial transformation of HUVEC remains to be further explored.

It has been demonstrated that EndMT is a dynamic biological process that can cause endothelial cell heterogeneity (Wu *et al*., 2019). However, this issue has not been studied in DN. RNA-sequencing technology is based on a high-throughput transcriptional sequencing method at the level of individual cells. By detecting differences in gene expression between individual cells, this can reveal the heterogeneity of tissues, organs, and cell clusters, decode the causes and processes of body lesions, and uncover relevant regulatory mechanisms (Bacher & Kendziorski, 2016; Luecken & Theis, 2019). Because of its unique advantages, single-cell sequencing has been applied to study the mechanism of EndMT in many diseases. In the study by Yan *et al*. (Luo *et al*., 2022), single-cell sequencing data of human brain tissue were used to study the process of EndMT blood–brain barrier dysfunction in multiple sclerosis, highlighting the functional role of EndMT in this disease. In addition, based on the pseudo-temporal developmental trajectory inference of endothelial cell subsets and differential gene screening, the transcription factor, ETS1, was identified as the central regulator of the EndMT process, promoting the development of precision therapy for multiple sclerosis. In the study by Monteiro *et al*. (2021), HUVEC were co-cultured with TGF-b2 and interleukin (IL)-1b *in vitro* to establish an EndMT model. These cells then underwent single-cell sequencing, and t-SNE dimensionality reduction clustering was performed on the data. The cell clusters in the model group were co-clustered into 11 clusters, in which the 1–6 clusters coincided with HUVEC of the control group, indicating that the 1–6 clusters showed the transcription characteristics of normal endothelial cells. The 7–11 clusters showed the down-regulated endothelial cell genome expression and transcriptional characteristics of mesenchymal cells, and also screened out novel long non-coding RNA transcriptional profiles related to EndMT processes.

Based on the above application of single-cell sequencing technology in disease research, this study used a bioinformatics analysis method to analyze the kidney single-cell sequencing data set of an online database in DN, explore the mechanism of renal EndMT in DN, and explore the relationship between FGFR1, a molecule with a strong role in marein signaling, and EndMT. A biogenic analysis of GSE131882 data set in a public database showed that renal cell populations were divided into 13 categories, of which endothelial cells could be further divided into five different subgroups, reflecting the heterogeneity of renal endothelial cells. The percentages of endothelial cell subsets in control and disease groups showed that, compared with the control group, the proportion of 0 subsets in the disease group was decreased, and the proportion of 2 and 4 subsets was increased. It was speculated that 0 subsets were control endothelial cell subsets, and 2 and 4 subsets were endothelial subsets with phenotypic changes. Pseudotemporal developmental track inference showed that the sequence of transition of endothelial cell subsets was $0 \rightarrow 1 \rightarrow 4 \rightarrow 2 \rightarrow 3$. A heatmap showed that expression of the mesenchymal marker proteins, VIM and FN1, increased in subsets 2 and 3, indicating that endothelial cell subsets transformed into mesenchymal phenotypes. Scatter plots showed increased FGFR1 expression during endothelial cell transformation into subgroups 2 and 3, suggesting that FGFR1 may positively correlate with EndMT. These studies indicate that EndMT exists in DN, renal endothelial cells are heterogeneous, and that the expression of FGFR1, a molecule that strongly interacts with marein, positively correlates with renal EndMT. In order to further verify the effect and mechanism of marein on EndMT, *in vitro* and *in vivo* experiments were conducted. We found that marein down-regulated the expression of FN1 and VIM in high glucose–treated endothelial cells, allowed endothelial cells to recover from a spindle to oval shape, and reduced cell mobility so as to inhibit high glucose–induced EndMT. In addition, marein reduced levels of fasting blood glucose, creatinine, and urea nitrogen in db/db mice, improved pathological renal structure, reduced collagen deposition in renal tissue, and reduced the expression of FN1 and VIM, suggesting that marein has an inhibitory effect on the EndMT of kidney cells in DKD.

The effect of Marein on FGFR1 and autophagy marker protein LC3II/I was studied in order to explore the mechanism of Marein on EndMT (Xie *et al*., 2020). FGFs/FGFR mechanisms have been shown to promote mesenchymal transition, secondary elevation of serum FGF23 levels is often detected in patients with chronic kidney disease, and elevated serum FGF23 concentrations can be used to predict the progression of kidney disease, especially in the early stages of diabetes (Goetz & Mohammadi, 2013). Moreover, secretion of FGF23 and FGF2 from renal endothelial cells, podocytes, mesangial cells, mesenchymal cells, and fibroblasts binds to FGFR1 receptors to promote the transition of endothelial cells and tubular epithelial cells into mesenchymal cells, thus accelerating the accumulation of renal mesangial cells and the generation of fibrotic lesions (Katoh *et al*., 2019; Geng *et al*., 2020). In our previous network pharmacological studies, we found that Marein has strong interaction with FGFR1, suggesting that FGFR1 may be the key molecule of Marein affecting EndMT in diabetic nephropathy (Li *et al*., 2022). Therefore, in this study, FGFR1 inhibitor AZD4547 was used to demonstrate the influence of FGFR1 on EndMT, helping to clarify the molecular mechanism of Marein inhibitory effect on EndMT. The results showed that AZD4547 intervention reduced the expression of FN1 and VIM when FGFR1 expression was suppressed, suggesting that FGFR1 inhibition could improve the high glucose-induced EndMT.

Autophagy is widely involved in various physiological and pathological processes of the body. It can degrade damaged cellular organelles, produce amino acids, free fatty acids and other substances, which can be reused by cells for protein and energy synthesis, so that cells can adapt to hypoxia and stress stimulation and other environments, which is conducive to cell survival (Maiuri *et al*., 2007; Levy *et al*., 2017; Nakatogawa, 2020). Studies have shown that autophagy is closely related to EndMT and fibrosis. When cells are stimulated by high glucose, oxidative stress and inflammation, it will cause dysfunction and aggregation of damaged organelles in the cell. Autophagy prevents matrix protein accumulation by removing protein polymers and damaged organelles. Insufficient autophagy will aggravate the deposition of cell matrix and promote the generation and development of fibrotic lesions ¡Error! No se encuentra el origen de la referencia.. Studies have shown that down-regulation of autophagy can lead to endothelial cell dysfunction in patients with type 2 diabetes (Takagaki *et al*., 2020). Moreover, experiments have shown that mice with endothelial cell-specific knockout of autophagy gene ATG5 will have reduced renal capillaries and glomerular lesions, and promote EndMT and renal dysfunction (Lenoir *et al*., 2015; Singh *et al*., 2015). It has also been proved that the first-line diabetes drug Metformin can inhibit the renal endothelial interstitial transformation and the generation of fibrosis through activating autophagy in diabetic nephropathy (Wang *et al*., 2021). Therefore, in order to explore whether Marein exerts its influence on high-glucose induced EndMT through activation of autophagy, the autophagy inhibitor 3-MA and Marein were used to intervene cells at the same time. The results showed that after autophagy inhibition, FN1 and VIM expressions were increased in the combined intervention group of 3-MA and Marein compared with the intervention group of Marein alone. Moreover, the expression of FGFR1 was also increased, indicating that Marein lost its inhibitory effect on the expressions of FN1 and VIM, that is, it could not reduce the expressions of mesenchymal marker proteins. Moreover, Marein also lost its inhibitory effect on FGFR1 expression after autophagy inhibition, suggesting that autophagy is very important for Marein to play the inhibitory effect on EndMT induced by high glucose. Marein may play a role in improving EndMT induced by high glucose by inducing autophagy and inhibiting FGFR1 expression.

CONCLUSIONS

Marein can improve the endothelial–mesenchymal transition of renal endothelial cells in diabetic nephropathy, and its mechanism maybe related to inducing autophagy and down-regulating FGFR1 expression.

Patient consent for publication. Single-cell RNA sequencing data were downloaded from the GEO database (GSE131882) from kidney tissue samples from kidney resection (each patient signed an informed consent and the experiment was approved by the Biomedical Research Ethics Committee of Southern Denmark in accordance with the Declaration of Helsinki).

ZHANG, F.; GUO, Q.; MAMAT, G.; TIAN, Y.; WANG, Q.; ZHANG, B. & LI, T. El papel de la mareína durante la transición endotelial-mesenquimatosa en la enfermedad renal diabética. *Int. J. Morphol., 42(4)*:1080-1095, 2024.

RESUMEN: La mareína es un compuesto flavonoide que reduce la glucosa y los lípidos en sangre y tiene un efecto protector en la diabetes. Sin embargo, no se han dilucidado el efecto y los mecanismos de la mareína sobre la transición endotelial-mesenquimatosa renal en la enfermedad renal diabética (ERD). En este estudio, los datos de secuenciación unicelular sobre DKD se analizaron utilizando un método de bioinformación y los datos se sometieron a una agrupación de dimensiones reducidas. Se descubrió que las células endoteliales podían dividirse en cinco subgrupos. La secuencia de desarrollo de los subgrupos fue 0, 1, 4, 2 y 3, de los cuales el subgrupo 3 tenía el fenotipo más intersticial. La expresión de la proteína marcadora mesenquimatosa: vimentina

(VIM), fibronectina (FN1) y receptor del factor de crecimiento de fibroblastos. 1 (FGFR1) aumentó con la conversión de subgrupos. En ratones db/db de 13 a 14 semanas de edad, que desarrollan complicaciones de DKD después de las 8 a 12 semanas de edad, la mareína redujo los niveles sanguíneos de glucosa, creatinina y nitrógeno ureico, mejoró el daño estructural en el tejido renal y redujo la deposición y expresión de colágeno de FN1 y VIM. Marein también aumentó el marcador de autofagia: Cadena ligera 3II/I (LC3II/I) y disminuyó la expresión de FGFR1 en el tejido renal. En un modelo de transición endotelial-mesenquimal, un nivel alto de glucosa indujo un cambio fenotípico en las células endoteliales de la vena umbilical humana. Marein disminuyó la migración de células endoteliales, mejoró la morfología de las células endoteliales y disminuyó la expresión de VIM y FN1. El uso del inhibidor de FGFR1, AZD4547, y del inhibidor de la autofagia, 3-metiladenina (3-MA), demostró aún más el efecto inhibidor de la mareína en la transición endotelial-mesenquimal inducida por niveles altos de glucosa al reducir la expresión de FGFR1 y regular positivamente la proteína marcadora de autofagia. , LC3II/I. En conclusión, este estudio sugiere que la mareína tiene un efecto protector sobre la transición endotelial-mesenquimatosa renal en la ERC, que puede estar mediada por la inducción de autofagia y la regulación negativa de la expresión de FGFR1.

PALABRAS CLAVE: Transición endotelial-mesénquimal; Marein; Enfermedad renal diabética; FGFR1; Autofagia.

REFERENCES

Bacher, R. & Kendziorski, C. Design and computational analysis of single-cell RNA-sequencing experiments. *Genome Biol., 17*:63, 2016.

Barry, D. M.; McMillan, E. A.; Kunar, B.; Lis, R.; Zhang, T.; Lu, T.; Daniel, E.; Yokoyama, M.; Gomez-Salinero, J. M.; Sureshbabu, A.; *et al*. Molecular determinants of nephron vascular specialization in the kidney. *Nat. Commun., 10(1)*:5705, 2019.

Baslan, T. & Hicks, J. Unravelling biology and shifting paradigms in cancer with single-cell sequencing. *Nat. Rev. Cancer, 17(9)*:557-69, 2017.

Chen, G.; Ning, B. & Shi, T. Single-cell RNA-Seq technologies and related computational data analysis. *Front. Genet., 10*:317, 2019.

Chen, L.; Shang, C.; Wang, B.; Wang, G.; Jin, Z.; Yao, F.; Yue, Z.; Bai, L.; Wang, R.; Zhao, S.; *et al*. HDAC3 inhibitor suppresses endothelial-to-mesenchymal transition via modulating inflammatory response in atherosclerosis. *Biochem. Pharmacol., 192*:114716, 2021.

DeFronzo, R. A.; Ferrannini, E.; Groop, L.; Henry, R. R.; Herman, W. H.; Holst, J. J.; Hu, F. B.; Kahn, C. R.; Raz, I.; Shulman, G. I.; *et al*. Type 2 diabetes mellitus. *Nat. Rev. Dis. Primers, 23*:1-15019, 2015.

Dias, T.; Bronze, M. R.; Houghton, P. J.; Mota-Filipe, H. & Paulo, A. The flavonoid-rich fraction of *Coreopsis tinctoria* promotes glucose tolerance regain through pancreatic function recovery in streptozotocin-induced glucose-intolerant rats. *J. Ethnopharmacol., 132(2)*:483-90, 2010.

Dias, T.; Liu, B.; Jones, P.; Houghton, P. J.; Mota-Filipe, H. & Paulo, A. Cytoprotective effect of *Coreopsis tinctoria* extracts and flavonoids on tBHP and cytokine-induced cell injury in pancreatic MIN6 cells. *J. Ethnopharmacol., 139(2)*:485-92, 2012.

Dumas, S. J.; Meta, E.; Borri, M.; Luo, Y.; Li, X.; Rabelink, T. J. & Carmeliet, P. Phenotypic diversity and metabolic specialization of renal endothelial cells. *Nat. Rev. Nephrol., 17(7)*:441-64, 2021.

Geng, L.; Lam, K. S. L. & Xu, A. The therapeutic potential of FGF21 in metabolic diseases: from bench to clinic. *Nat. Rev. Endocrinol., 16(11)*:654-67, 2020.

Gilbert, R. E. The endothelium in diabetic nephropathy. *Curr. Atheroscler. Rep., 16(5)*:410, 2014.

Goetz, R. & Mohammadi, M. Exploring mechanisms of FGF signalling through the lens of structural biology. *Nat. Rev. Mol. Cell Biol., 14(3)*:166-80, 2013.

Guo, Y.; Ran, Z.; Zhang, Y.; Song, Z.; Wang, L.; Yao, L.; Zhang, M.; Xin, J. & Mao, X. Marein ameliorates diabetic nephropathy by inhibiting renal sodium glucose transporter 2 and activating the AMPK signaling pathway in db/db mice and high glucose-treated HK-2 cells. *Biomed. Pharmacother., 131*:110684, 2020.

Jourde-Chiche, N.; Fakhouri, F.; Dou, L.; Bellien, J.; Burtey, S.; Frimat, M.; Jarrot, P. A.; Kaplanski, G.; Le Quintrec, M.; Pernin, V.; *et al*. Endothelium structure and function in kidney health and disease. *Nat. Rev. Nephrol., 15(2)*:87-108, 2019.

Kalantar-Zadeh, K.; Jafar, T. H.; Nitsch, D.; Neuen, B. L. & Perkovic, V. Chronic kidney disease. *Lancet, 398(10302)*:786-802, 2021.

Katoh, M. Fibroblast growth factor receptors as treatment targets in clinical oncology. *Nat. Rev. Clin. Oncol., 16(2)*:105-22, 2019.

Kuppe, C.; Ibrahim, M. M.; Kranz, J.; Zhang, X.; Ziegler, S.; Perales-Patón, J.; Jansen, J.; Reimer, K. C.; Smith, J. R.; Dobie, R.; *et al*. Decoding myofibroblast origins in human kidney fibrosis. *Nature, 589(7841)*:281-6, 2021.

Lassén, E. & Daehn, I. S. Molecular mechanisms in early diabetic kidney disease: glomerular endothelial cell dysfunction. *Int. J. Mol. Sci., 21(24)*:9456, 2020.

Lenoir, O.; Jasiek, M.; Hénique, C.; Guyonnet, L.; Hartleben, B.; Bork, T.; Chipont, A.; Flosseau, K.; Bensaada, I.; Schmitt, A.; *et al*. Endothelial cell and podocyte autophagy synergistically protect from diabetes-induced glomerulosclerosis. *Autophagy, 11(7)*:1130-45, 2015.

Levy, J. M. M.; Towers, C. G. & Thorburn, A. Targeting autophagy in cancer. *Nat. Rev. Cancer, 17(9)*:528-42, 2017.

Li, T.; Liu, S.; Abula, Z.; Kadier, K.; Guo, Y.; Gu, S.; Wang, L.; Zhang, F.; Mao, X. & Li, X. Mechanisms of *Coreopsis tinctoria* Nutt in the treatment of diabetic nephropathy based on network pharmacology analysis of its active ingredients. *Int. J. Morphol., 40(5)*:1152-64, 2022.

Liu, W. J.; Huang, W. F.; Ye, L.; Chen, R. H.; Yang, C.; Wu, H. L.; Pan, Q. J. & Liu, H. F. The activity and role of autophagy in the pathogenesis of diabetic nephropathy. *Eur. Rev. Med. Pharmacol. Sci., 22(10)*:3182-9, 2018.

Luecken, M. D. & Theis, F. J. Current best practices in single-cell RNA-seq analysis: a tutorial. *Mol. Syst. Biol., 15(6)*:e8746, 2019.

Luo, Y.; Yang, H.; Wan, Y.; Yang, S.; Wu, J.; Chen, S.; Li, Y.; Jin, H.; He, Q.; Zhu, D. Y.; *et al*. Endothelial ETS1 inhibition exacerbate blood-brain barrier dysfunction in multiple sclerosis through inducing endothelial-to-mesenchymal transition. *Cell Death Dis., 13(5)*:462, 2022.

Maiuri, M. C.; Zalckvar, E.; Kimchi, A. & Kroemer, G. Self-eating and self-killing: crosstalk between autophagy and apoptosis. *Nat. Rev. Mol. Cell Biol., 8(9)*:741-52, 2007.

Monteiro, J. P.; Rodor, J.; Caudrillier, A.; Scanlon, J. P.; Spiroski, A. M.; Dudnakova, T.; Pflüger-Müller, B.; Shmakova, A.; von Kriegsheim, A.; Deng, L.; *et al*. MIR503HG loss promotes endothelial-to-mesenchymal transition in vascular disease. *Circ. Res., 128(8)*:1173-90, 2021.

Nakatogawa, H. Mechanisms governing autophagosome biogenesis. *Nat. Rev. Mol. Cell Biol., 21(8)*:439-58, 2020.

Niu, G.; Zhou, M.; Wang, F.; Yang, J.; Huang, J. & Zhu, Z. Marein ameliorates Ang II/hypoxia-induced abnormal glucolipid metabolism by modulating the HIF-1a/PPARa/g pathway in H9c2 cells. *Drug Dev. Res., 82(4)*:523-32, 2021.

Reidy, K.; Kang, H. M.; Hostetter, T. & Susztak, K. Molecular mechanisms of diabetic kidney disease. *J. Clin. Invest., 124(6)*:2333-40, 2014.

Saelens, W.; Cannoodt, R.; Todorov, H. & Saeys, Y. A comparison of single-cell trajectory inference methods. *Nat. Biotechnol., 37(5)*:547-54, 2019.

Singh, K. K.; Lovren, F.; Pan, Y.; Quan, A.; Ramadan, A.; Matkar, P. N.; Ehsan, M.; Sandhu, P.; Mantella, L. E.; Gupta, N.; *et al*. The essential autophagy gene ATG7 modulates organ fibrosis via regulation of endothelial-to-mesenchymal transition. *J. Biol. Chem., 290(5)*:2547-59, 2015.

Takagaki, Y.; Lee, S. M.; Dongqing, Z.; Kitada, M.; Kanasaki, K. & Koya, D. Endothelial autophagy deficiency induces IL6 - dependent endothelial mesenchymal transition and organ fibrosis. *Autophagy, 16(10)*:1905-14, 2020.

Wang, F.; Sun, H.; Zuo, B.; Shi, K.; Zhang, X.; Zhang, C. & Sun, D. Metformin attenuates renal tubulointerstitial fibrosis via upgrading autophagy in the early stage of diabetic nephropathy. *Sci. Rep., 11(1)*:16362, 2021.

Wilson, P. C.; Wu, H.; Kirita, Y.; Uchimura, K.; Ledru, N.; Rennke, H. G.; Welling, P. A.; Waikar, S. S. & Humphreys, B. D. The single-cell transcriptomic landscape of early human diabetic nephropathy. *Proc. Natl. Acad. Sci. U. S. A., 116(39)*:19619-25, 2019.

Wu, H.; Kirita, Y.; Donnelly, E. L. & Humphreys, B. D. Advantages of single-nucleus over Single-Cell RNA sequencing of adult kidney: rare cell types and novel cell states revealed in fibrosis. *J. Am. Soc. Nephrol., 30(1)*:23-32, 2019.

Xie, Y.; Su, N.; Yang, J.; Tan, Q.; Huang, S.; Jin, M.; Ni, Z.; Zhang, B.; Zhang, D.; Luo, F.; *et al*. FGF/FGFR signaling in health and disease. *Signal Transduct. Target Ther., 5(1)*:181, 2020.

Xu, S.; Ilyas, I.; Little, P. J.; Li, H.; Kamato, D.; Zheng, X.; Luo, S.; Li, Z.; Liu, P.; Han, J.; *et al*. Endothelial dysfunction in atherosclerotic cardiovascular diseases and beyond: from mechanism to pharmacotherapies. *Pharmacol. Rev., 73(3)*:924-67, 2021.

Yao, L.; Li, J.; Li, L.; Li, X.; Zhang, R.; Zhang, Y. & Mao, X. *Coreopsis tinctoria* Nutt ameliorates high glucose-induced renal fibrosis and inflammation via the TGF-b1/SMADS/AMPK/NF-kB pathways. *BMC Complement. Altern. Med., 19(1)*:14, 2019.

Corresponding author:
Fang Zhang
Department of Histology and Embryology
School of Basic Medical Sciences
Xinjiang Medical University
Urumqi Xinjiang
830011
CHINA

E-mail: zf1925985782@163.com